

Memory and aging effect in hierarchical spin orderings of stage-2 CoCl₂ graphite intercalation compound

Masatsugu Suzuki* and Itsuko S. Suzuki†

Department of Physics, State University of New York at Binghamton, Binghamton, New York 13902-6000

Motohiro Matsuura

*Department of Management and Information Science,
Fukui University of Technology, Fukui, Fukui 910-8505, JAPAN*

(Dated: November 11, 2018)

Stage-2 CoCl₂ graphite intercalation compound undergoes two magnetic phase transitions at T_{cl} (= 7.0 K) and T_{cu} (= 8.9 K). The aging dynamics of this compound is studied near T_{cl} and T_{cu} . The intermediate state between T_{cl} and T_{cu} is characterized by a spin glass phase extending over ferromagnetic islands. A genuine thermoremanent magnetization (TRM) measurement indicates that the memory of the specific spin configurations imprinted at temperatures between T_{cl} and T_{cu} during the field-cooled (FC) aging protocol can be recalled when the system is re-heated at a constant heating rate. The zero-field cooled (ZFC) and TRM magnetization is examined in a series of heating and reheating process. The magnetization shows both characteristic memory and rejuvenation effects. The time (t) dependence of the relaxation rate $S_{ZFC}(t) = (1/H)dM_{ZFC}(t)/d\ln t$ after the ZFC aging protocol with a wait time t_w , exhibits two peaks at characteristic times t_{cr1} and t_{cr2} between T_{cl} and T_{cu} . An aging process is revealed as the strong t_w dependence of t_{cr2} . The observed aging and memory effect is discussed in terms of the droplet model.

PACS numbers: 75.40.Gb, 75.50.Lk, 75.30.Kz, 75.30.GW

I. INTRODUCTION

Magnetic phase transitions of stage-2 CoCl₂ graphite intercalation compound (GIC) have been extensively studied.^{1,2,3,4,5,6,7,8,9,10,11} This compound magnetically behaves like a quasi two-dimensional (2D) XY-like ferromagnet with a very weak antiferromagnetic interplanar interaction. The intercalate layers are formed of small islands whose average diameters are on the order of 450 Å. The peripheral chlorine ions at the island boundary provide acceptor sites for charges transferred from the graphite layer to the intercalate layer. This compound undergoes magnetic phase transitions at T_{cu} (= 8.9 K) and T_{cl} (= 7.0 K). The growth of the in-plane spin correlation length ξ_a is limited by the existence of the islands, making the effective interplanar exchange interaction finite and suppressing the 3D spin ordering to a lower temperature than T_{cu} . At T_{cu} a 2D ferromagnetic spin order develops inside each island. Between T_{cl} and T_{cu} the 2D ferromagnetic long range order (LRO) is established. The in-plane spin correlation length grows to the order of the island size at T_{cl} . Below T_{cl} the system is in a 3D antiferromagnetic phase with the 2D ferromagnetic layers being stacked antiferromagnetically along the c axis.

However, it seems that such a simple picture for the ordering process below T_{cu} , is not appropriate for the peculiar phenomena observed so far in stage-2 CoCl₂ GIC,^{3,5,7,8,9} which is rather characteristic of the spin glass (SG) phase. Further it may be also inconsistent with the following experimental results. (i) The absorption χ'' shows peaks at T_{cl} and T_{cu} . The peak at T_{cl} shifts to the high- T side with increasing f , while the peak at T_{cu} remains unshifted.¹⁰ (ii) The spin correlation length

along the c axis, ξ_c , grows rapidly below T_{cu} but quickly saturates to a constant value of 22 Å, or less than two magnetic layers (the c -axis repeat distance $d = 12.70\text{Å}$).⁴ Below T_{cl} a 3D antiferromagnetic long range order (LRO) is established mainly through effective interplanar interactions including interisland interactions between islands in adjacent intercalate layers.

Under such a circumstance, we performed a series of experiments on the dynamical aspect of the ordering process. Most of them are used to study the aging dynamics (aging, memory and rejuvenation) of SG's. In this paper we study the aging dynamics of stage-2 CoCl₂ GIC near T_{cu} and T_{cl} . Our experiments include (i) genuine thermoremanent magnetization (TRM), (ii) relaxation rate of the ZFC susceptibility, (iii) zero-field cooled (ZFC) magnetization and TRM magnetization in a series of heating and cooling process which is the same procedure used by Matsuura et al.⁵ for stage-2 CoCl₂ GIC, and (iv) field-cooled magnetization in a FC cooling protocol (with an intermittent stop for a wait time in the absence of a magnetic field) which is the same protocol used by Sun et al.¹² for permalloy (Ni₈₁Fe₁₉) nanoparticles.

We show that the intermediate state is a SG ordered phase extending over ferromagnetic islands. The magnetization shows both characteristic memory and rejuvenation effects. The time (t) dependence of the relaxation rate $S_{ZFC}(t) = (1/H)dM_{ZFC}(t)/d\ln t$ after the ZFC aging protocol with a wait time t_w , exhibits two peaks at characteristic times t_{cr1} and t_{cr2} between T_{cl} and T_{cu} . An aging process is revealed as the strong t_w dependence of t_{cr2} . The observed aging and memory effect will be discussed in terms of the droplet model.^{13,14,15}

II. EXPERIMENTAL PROCEDURE

A stage-2 CoCl_2 GIC sample was prepared by intercalation of pristine CoCl_2 into a single crystal of kish graphite in a Cl_2 gas atmosphere at 740 Torr for three weeks at 540 °C. The sample used in the present experiment is one used in the previous experiments.^{10,11} The DC magnetization and AC magnetic susceptibility were measured using a SQUID magnetometer (Quantum Design, MPMS XL-5) with an ultra low field capability option. Before the measurement, a remnant magnetic field was reduced to zero field (exactly less than 3 mOe) at 298 K. We measured the DC magnetization as a function of temperature after various kinds of cooling protocol. The detail of the cooling protocol for each experiment will be presented in Sec. III. We also measured the time dependence of the ZFC magnetization at various wait times.

III. RESULT

A. T dependence of M_{ZFC} , M_{FC} , M_{TRM} , M_{IRM} and ΔM ($= M_{FC} - M_{ZFC}$)

In the previous paper,¹⁰ we have studied the dynamic aspect of in-plane spin ordering in stage-2 CoCl_2 GIC from both the dispersion χ' and absorption χ'' at $f = 0.1$ Hz acquired using an AC magnetic susceptibility. The absorption χ'' shows three peaks at $T = T_{cu}$ ($= 8.9$ K), T_{p1} ($= 8.4$ K), and T_{cl} ($= 7.0$ K), while χ' has a single peak at T_{p1} . These results indicate that this compound undergoes two magnetic phase transitions at T_{cl} and T_{cu} .

In order to see how these successive magnetic phase transitions are observed in the DC magnetic susceptibility, we measured the temperature (T) dependence of the magnetization M_{ZFC} , M_{FC} , and M_{TRM} in the case of $H = 1$ and 0.15 Oe. (a) *The zero-field cooled magnetization (M_{ZFC}) measurement.* The system was annealed at 50 K for 1200 sec in the absence of H . The system was cooled from 50 to 1.9 K at $H = 0$ (ZFC aging protocol). After the system was aged at 1.9 K for $t_w = 100$ sec at $H = 0$, the magnetic field is applied at H ($= 1$ and 0.15 Oe). Subsequently M_{ZFC} was measured with increasing T from 1.9 to 12 K at the rate of 0.025 K/minute. (b) *The field cooled magnetization (M_{FC}) measurement.* The system was annealed at 50 K for 1200 sec in the presence of H ($= 1$ and 0.15 Oe). Then the system was cooled from 50 to 12 K in the presence of H (FC aging protocol). The magnetization M_{FC} was measured with decreasing T from 12 to 1.9 K. (c) *The thermoremanent magnetization (M_{TRM}) measurement.* The system was cooled from 50 to 1.9 K in the presence of $H = H_c$ ($= 1$ and 0.15 Oe) through the FC aging protocol. After the system was aged at 1.9 K for $t_w = 100$ sec, the field was cut off ($H = 0$). Then the magnetization M_{TRM} was measured with increasing T from 1.9 to 12 K.

Figure 1(a) shows the T dependence of M_{ZFC} , M_{FC} , M_{TRM} , and $\Delta M = M_{FC} - M_{ZFC}$ for $H = 1$ Oe. The

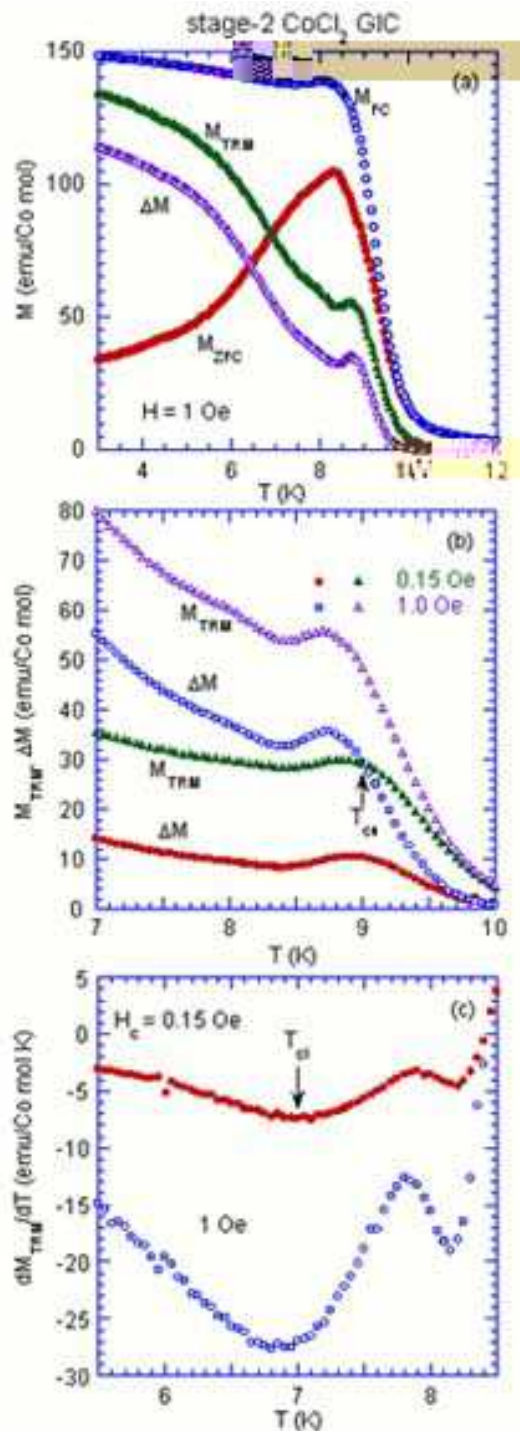


FIG. 1: (Color online) (a) T dependence of M_{ZFC} , M_{FC} , M_{TRM} and ΔM ($= M_{FC} - M_{ZFC}$) for stage-2 CoCl_2 GIC. $H = 1$ Oe. (b) T dependence of M_{TRM} at $H_c = 1$ and 0.15 Oe and ΔM at $H = 1$ and 0.15 Oe. $T_{cu} = 8.9$ K (denoted by arrow). (c) T dependence of dM_{TRM}/dT at $H_c = 1$ and 0.15 Oe. $T_{cl} = 7.0$ K (denoted by arrow).

magnetization M_{ZFC} exhibits a peak at 8.3 K close to T_{p1} , which remains unchanged with decreasing H from 1 to 0.15 Oe. The deviation of M_{ZFC} from M_{FC} starts to occur below 10.5 K, due to the irreversibility effect of magnetization. Figure 1(b) shows the T dependence of M_{TRM} for $H_c = 0.15$ and 1 Oe, and ΔM for $H = 0.15$ and 1 Oe. The magnetization M_{TRM} at $H_c = 1$ Oe exhibits a local maximum at 8.70 K. The local-maximum temperature increases with decreasing H_c and reaches 8.85 K at $H_c = 0.15$, which is very close to T_{cu} . Although ΔM at $H = H_0$ ($= 0.15$ and 1 Oe) is smaller than M_{TRM} at $H_c = H_0$, below 10 K, the T dependence of ΔM at $H = H_0$ is similar to that of M_{TRM} at $H = H_0$. Figure 1(c) shows the T dependence of dM_{TRM}/dT at $H_c = 1$ and 0.15 Oe. The derivative dM_{TRM}/dT exhibits a negative local minimum at $T = 6.9$ K for $H_c = 1$ Oe and at $T = T_{cu}$ ($= 7.0$ K) for $H_c = 0.15$ Oe.

B. Genuine TRM measurement

We present a memory effect observed in the so-called genuine TRM magnetization measurement of stage-2 CoCl_2 GIC. Similar behavior is observed in SG's.^{16,17,18,19} Our system was cooled from 50 K to an intermittent stop temperature T_s ($6 \leq T_s \leq 9.1$ K) in the presence of $H = H_c$ ($= 1$ Oe) (stop-wait process). The system was aged at T_s for a wait time t_s ($= 1.0 \times 10^4$ sec) at $H = H_c$, and subsequently it was cooled again down to 3.0 K. After the magnetic field was switched off at 3 K, the TRM magnetization was measured with increasing T from 3.0 to 12.0 K at $H = 0$. This value of the TRM magnetization is compared with that of the TRM magnetization which was measured with increasing T after the FC cooling protocol without any stop-wait process [$M_{TRM}^{ref}(T)$ as the reference curve]. Here we define the difference $\Delta M_{TRM}(T; T_s, t_s)$ as

$$\Delta M_{TRM}(T, T_s, t_s) = M_{TRM}(T; T_s, t_s) - M_{TRM}^{ref}(T). \quad (1)$$

Figure 2 shows the T dependence of $M_{TRM}(T)(T; T_s, t_s)$ (stop-wait curve) and $M_{TRM}^{ref}(T)$ (reference curve) at $t_s = 1.0 \times 10^4$ sec for typical stop temperatures ($T_s = 6.6, 7.2, 8.0,$ and 8.5 K). The reference curve and the stop-wait curves coalesce at low temperatures and only start to deviate as T_s is approached from the low T side. The stop-wait curve lie significantly above the reference curve in the vicinity of T_s . Figure 3 shows the T dependence of $\Delta M_{TRM}(T; T_s, t_s)$ at various T_s . The difference $\Delta M_{TRM}(T; T_s, t_s)$ shows either a symmetric broad peak centered at $T = T_s$ for $T_s < 7.4$ K or an asymmetric cusp centered at $T = T_s$ for $7.6 \text{ K} < T < T_{cu}$. The peak of $\Delta M_{TRM}(T; T_s, t_s)$ is not observed for $T_s \leq 6$ K. The result indicates that the spin configuration imprinted at T_s is recovered on reheating. In this sense, the system sustains a memory of an equilibrium state reached after a stop-wait process at T_s . Such phenomena are commonly observed in various kinds of SG's. Figure

4(a) shows the T_s dependence of the peak height of the curve $\Delta M_{TRM}(T; T_s, t_s)$ vs T located at T_s , [denoted by $(\Delta M_{TRM})_{max}$]. The peak height exhibits a sharp peak at $T_s = T_{cl}$. It decreases with further increasing T_s and tends to zero around T_{cu} . As will be discussed in Sec. IV C, the magnetization $(\Delta M_{TRM})_{max}$ is roughly proportional to ξ_a^2 between T_{cl} and T_{cu} . The increase of $(\Delta M_{TRM})_{max}$ with decreasing T between T_{cl} and T_{cu} suggests that ξ_a increases with decreasing T from T_{cu} to T_{cl} . Figure 4(b) shows the T_s dependence of the full-width at half-maximum [$= (\Delta T)_{FWHM}$] for the peak of the curve ΔM_{TRM} vs T located at $T = T_s$. The full-width at half-maximum $(\Delta T)_{FWHM}$ exhibits a peak around $T_s = T_{cl}$. It is on the order of 1.2 K at $T_s = T_{cl}$ and 0.4 K around $T_s = T_{cu}$. The T_s dependence of $(\Delta T)_{FWHM}$ will be discussed in terms of the overlap length of the droplet model^{13,14,15} for SG's in Sec. IV D.

C. Relaxation rate $S_{ZFC}(t)$

We have measured the t dependence of M_{ZFC} at the fixed T for various wait time t_w [$= (0.2 - 3) \times 10^4$ sec], where $H = 1$ Oe. The measurement was carried out after the ZFC aging protocol: annealing of the system at $T = 50$ K and $H = 0$ for 1.2×10^3 sec, quenching from 50 K to T at $H = 0$, and isothermal aging at T for t_w . The origin of t ($t = 0$) is a time just after $H = 1$ Oe is applied at T . We find that M_{ZFC} increases with increasing t , depending on t_w and T . Figure 5(a) shows the t dependence of the relaxation rate $S_{ZFC}(t)$ at various T , where $t_w = 3.0 \times 10^4$ sec. Below $T = 7.5$ K, $S_{ZFC}(t)$ exhibits a kink at a characteristic time $t_{cr1} \approx (2.06 - 2.59) \times 10^3$ sec and a very broad peak at a characteristic time $t_{cr2} \approx (2.02 - 2.80) \times 10^4$ sec. At $T = 8.5$ and 9.0 K, $S_{ZFC}(t)$ has two broad peaks at $t = t_{cr1}$ and t_{cr2} . Figure 5(b) shows the T dependence of t_{cr1} and t_{cr2} thus obtained. The characteristic time t_{cr1} slightly decreases with increasing T . The characteristic time t_{cr2} exhibits a peak around 8 K, and decreases with further increasing T . This suggests that the ordered SG phase extending over islands tends to vanish with increasing T , in association with the disappearance of the ferromagnetic order in each island above T_{cu} .

Figure 6(a) shows the t dependence of $S_{ZFC}(t)$ for different t_w at $T = 7.0$ K, where $H = 1$ Oe. The t dependence of $S_{ZFC}(t)$ is strongly dependent on t_w . For $t_w = 2.0 \times 10^3$ sec, $S_{ZFC}(t)$ has a peak at $t = t_{cr1} = t_{cr2} = 2.1 \times 10^3$ sec which is very close to t_w . For $t_w = 1.0 \times 10^4$ sec, $S_{ZFC}(t)$ has a kink at $t = t_{cr1} = 2.1 \times 10^3$ sec and a very broad peak at $t = t_{cr2} = 6.9 \times 10^3$ sec. For $t_w = 3 \times 10^4$ sec, $S_{ZFC}(t)$ has a kink at $t = t_{cr1} = 2.1 \times 10^3$ sec and a very broad peak at $t_{cr2} = 2.04 \times 10^4$ sec. The time t_{cr1} is independent of t_w and nearly equal to 2.1×10^3 sec, while the time t_{cr2} is linearly dependent on t_w : $t_{cr2}/t_w = 0.68 \pm 0.02$. The shift of the peak of $S_{ZFC}(t)$ at t_{cr2} with increasing t_w to the long- t side reflects the influence of the aging process

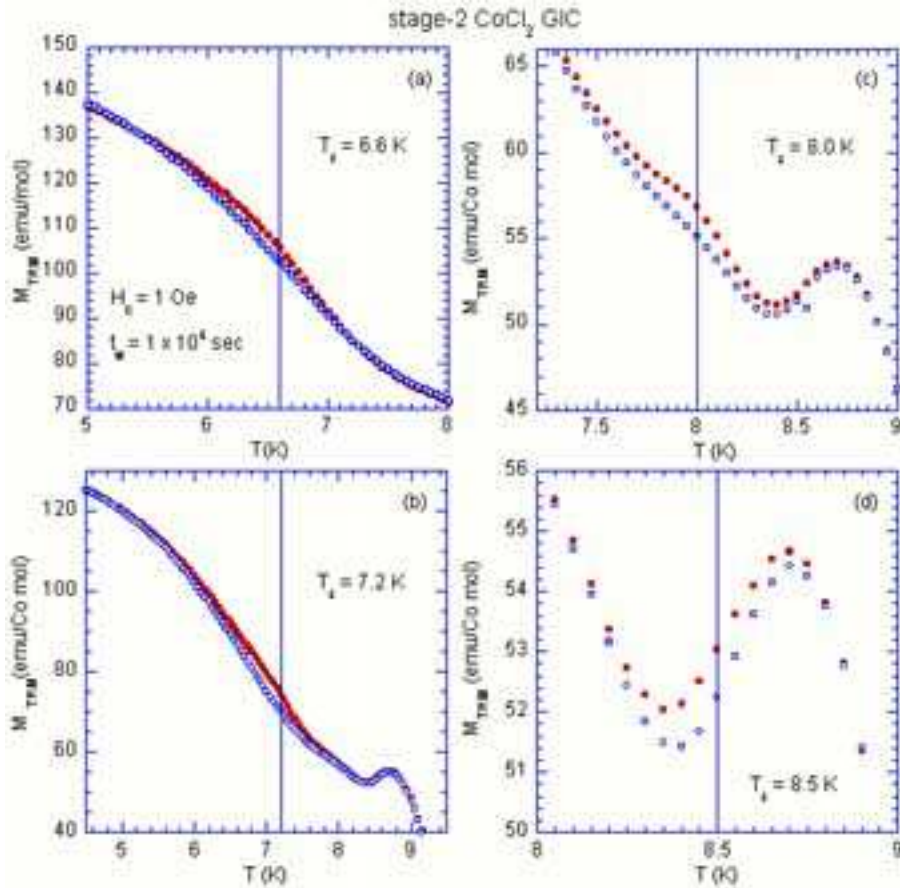


FIG. 2: (Color online) T dependence of $M_{TRM}(T; T_s, t_s)$ (closed circles) and of $M_{TRM}^{ref}(T)$ (open circles). $M_{TRM}(T; T_s, t_s)$ is measured with increasing T at $H = 0$ after the FC cooling protocol at $H_c = 1$ Oe with a stop-wait at T_s for $t_s = 1.0 \times 10^4$ sec. M_{TRM}^{ref} is measured with increasing T after the FC cooling protocol at $H_c = 1$ Oe without such a stop-wait protocol. (a) $T_s = 6.6$ K, (b) 7.2 K, (c) 8.0 K, and (d) 8.5 K.

on the behavior of the relaxation of the system at $T = 7$ K, where $t_{cr2} < t_w$. Figure 6(b) shows the t dependence of $S_{ZFC}(t)$ for different t_w at $T = 8.0$ K, where $H = 1$ Oe. The relaxation rate $S_{ZFC}(t)$ exhibits two broad peaks at $t = t_{cr1}$ and t_{cr2} for $t_w = 5.0 \times 10^3$, 1.0×10^4 , and 3.0×10^4 sec. The time t_{cr1} is independent of t_w and is nearly equal to 2.0×10^3 sec, while the time t_{cr2} is linearly dependent on t_w : $t_{cr2}/t_w = 1.123 \pm 0.002$. The latter behavior is due to the influence of aging process on the behavior of the relaxation at $T = 8$ K, where $t_{cr2} > t_w$. These aging phenomena suggest that two kinds of ordered domains coexists in the intermediate state. The detail will be discussed in Sec. IV B.

D. Memory effect for M_{TRM} and M_{ZFC}

Here we present our result on memory phenomena of M_{TRM} and M_{ZFC} for stage-2 CoCl_2 GIC, which is observed in a series of heating and cooling processes. Such a characteristic phenomenon has been predicted theoretically in SG based on a successive bifurcation model of the

energy level scheme below the spin freezing temperature.⁵

(i) *TRM case.* Before the TRM magnetization measurement, a field cooling (FC) protocol was carried out, consisting of (a) annealing of the system at 50 K for 1200 sec in the presence of H ($= 1$ or 0.15 Oe), (b) quenching of the system from 50 K to $T = T_i = 3$ K, and (c) aging the system at $T = T_i$ at H for a wait time $t_w = 100$ sec. Just after the magnetic field was turned off, the TRM magnetization was measured with increasing T from T_i ($= 3$ K) to T_1 ($= 4.5$ K) (the first U-turn temperature) and subsequently with decreasing T from T_1 to T_i . (the cooling process). In turn, it was measured with increasing T from T_i to T_2 ($= 5.0$ K) (the heating process) and subsequently with decreasing T from T_2 to T_i (the cooling process). This process was repeated for the U-turn temperatures T_r ($r = 3-11$), where $T_r > T_i$. The schematic diagram of these processes for the TRM measurement is also shown in Fig. 7(a).

Figures 8 and 9 show typical examples of the T dependence of M_{TRM} obtained using the above procedure, where $H = 1$ Oe (Figs. 8(a) and (b)) and $H = 0.15$ Oe (Figs. 9(a) and (b)). The value of M_{TRM} lies between

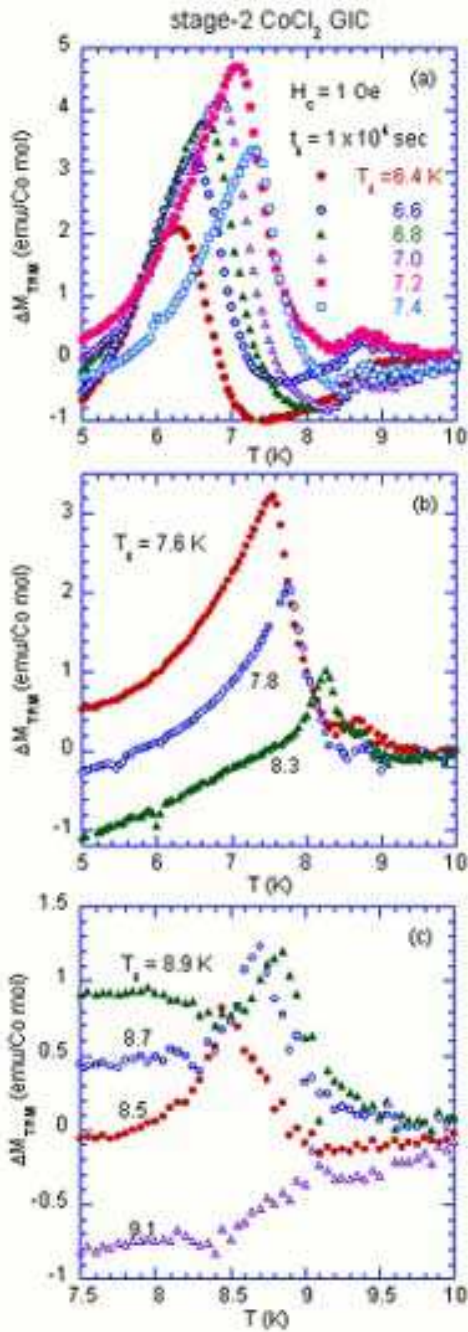


FIG. 3: (Color online) T dependence of $\Delta M_{TRM}(T; T_s, t_s) [= M_{TRM}(T; T_s, t_s) - M_{TRM}^{ref}(T)]$. $t_s = 1.0 \times 10^4$ sec. $6.4 \leq T_s \leq 9.1$ K. $H_c = 1$ Oe. (a) $6.6 \leq T \leq 7.4$ K. (b) $7.6 \leq T \leq 8.3$ K. (c) $8.5 \leq T \leq 9.1$ K.

those of M_{TRM}^{ref} and M_{IRM}^{ref} (the reference curves) at any T below T_{cu} . Here the magnetization M_{TRM}^{ref} is measured with increasing T from T_i to 12 K at $H = 0$ after the FC cooling protocol at $H = 1$ Oe. The magnetization M_{IRM}^{ref} is measured with increasing T from T_i to 12 K at $H = 0$ after the ZFC cooling protocol from 12 K to T_i , switching H from 0 to 1 Oe, aging the system

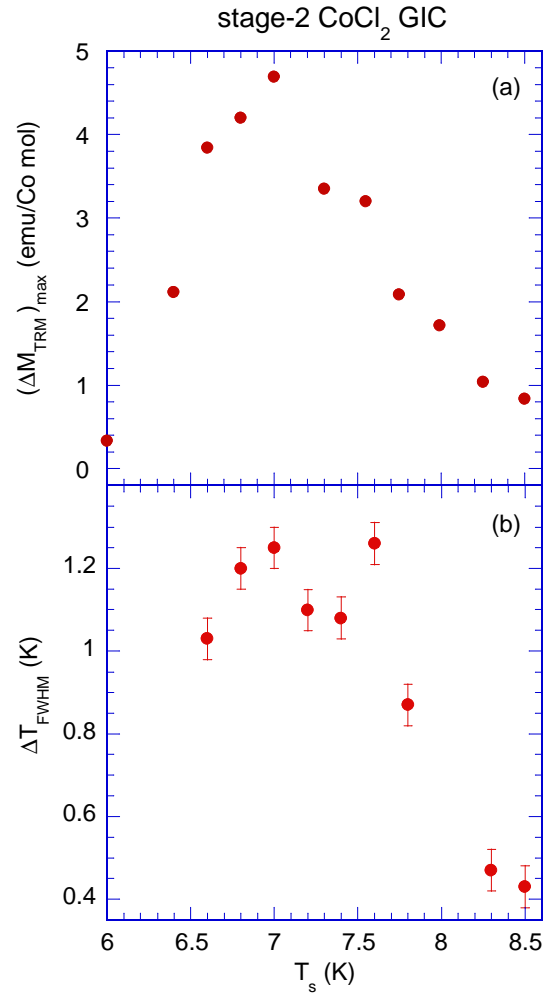


FIG. 4: (Color online) (a) T_s dependence of the peak height of $\Delta M_{TRM}(T; T_s, t_s)$ denoted by $(\Delta M_{TRM})_{max}$. The curve of ΔM_{TRM} vs T shows a peak at T_s . (b) T_s dependence of the full-width at half-maximum ($= \Delta T_{FWHM}$) for the peak of the curve of ΔM_{TRM} vs T located at $T = T_s$.

at $H = 1$ Oe for a wait time $t_w = 100$ sec, and again switching H from 1 Oe to 0. Figure 10 shows typical examples of the path of M_{TRM} vs T obtained in both the cooling process ($T = T_r \rightarrow T_i$) and the heating process ($T = T_i \rightarrow T_r$), where $T_r = 7.0, 7.4, 7.8, 8.2, 8.6, 8.6,$ and 8.9 K. Figure 11 (a) shows the T_r dependence of M_r and M_i , where M_r and M_i are the values of M_{TRM} at $T = T_r$ and T_i in the cooling process ($T = T_r \rightarrow T_i$), respectively. Figure 11(b) shows the T_r dependence of the derivative dM_i/dT_r . It exhibits a negative local minimum at $T_r = T_{cl} = 7$ K. Figure 11(c) shows the difference $\Delta M_{ir}^{TRM} (= M_i - M_r)$ which is derived from Fig. 11(a). For $T_r < 7.0$ K, the path of $M_{TRM}(T \downarrow)$ in the cooling process ($T = T_r \rightarrow T_i$) is almost the same as that of $M_{TRM}(T \uparrow)$ in the heating process ($T = T_i \rightarrow T_r$), indicating that M_{TRM} vs T curve is reversible on cooling and heating. For $T_r \geq 7.8$ K, however, the M_{TRM} vs T curve is irreversible in the cooling and heating processes.

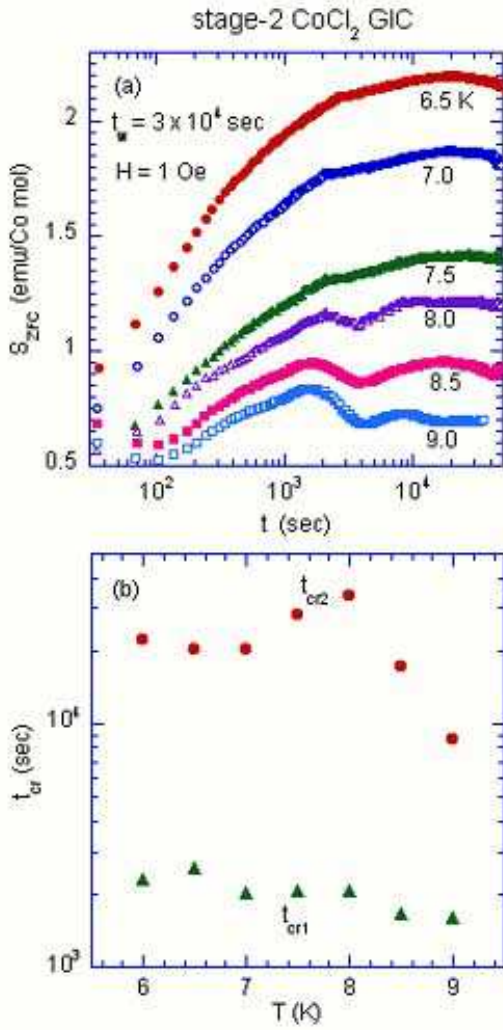


FIG. 5: (Color online) (a) t dependence of the relaxation rate $S_{ZFC}(t) [= (1/H)dM_{ZFC}(t)/d\ln t]$. $M_{ZFC}(t)$ was measured at a fixed T as a function of t after the ZFC cooling protocol consisting of the cooling from 50 K to T at $H = 0$ and the annealing at T for a wait time $t_w = 3.0 \times 10^4$ sec. $T = 6.5 - 9.0$ K. $t = 0$ is a time at which the field ($H = 1$ Oe) is applied after the wait time. (b) T dependence of the times t_{cr1} (closed triangles) and t_{cr2} (closed circles) for $t_w = 3.0 \times 10^4$ sec, where $S_{ZFC}(t)$ has either a peak or kink at $t = t_{cr1}$ and t_{cr2} as shown in Fig. 5(a). $H = 1$ Oe.

For $T_r = 8.6$ and 8.9 K, the curve of M_{TRM} vs T shows a broad peak around T_{cl} and a local minimum between T_{cl} and T_{cu} in both the cooling and heating process between T_{cl} and T_{cu} . Figure 12(a) shows the difference $\Delta M_{TRM} [= M_{TRM}(T\uparrow) - M_{TRM}(T\downarrow)]$ as a function of T for various T_r . The difference ΔM_{TRM} exhibits a positive peak at a characteristic temperature T_p^{TRM} below T_r . The peak temperature T_p^{TRM} linearly increases with increasing T_r through the relation $T_p^{TRM} - T_r = 0.3$ K for $7.8 \leq T_r \leq 8.9$ K.

The intermediate state between T_{cl} and T_{cu} has charac-

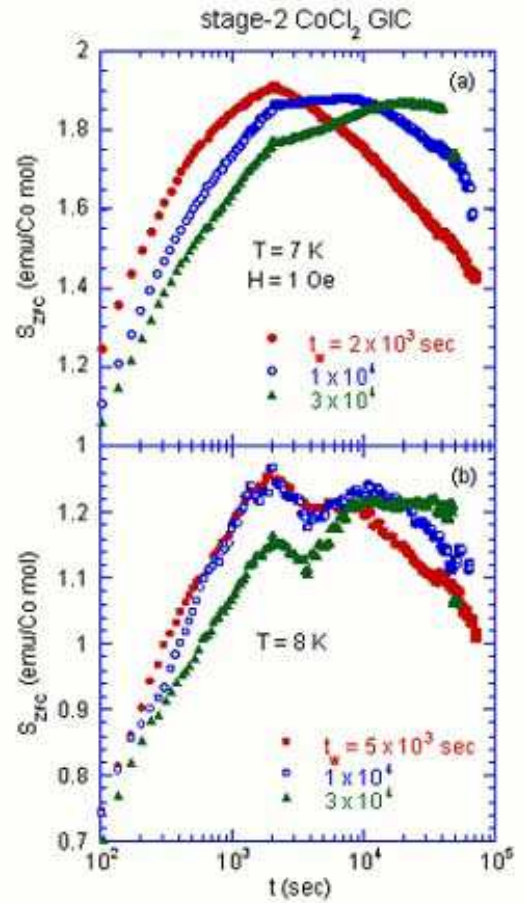


FIG. 6: (Color online) t dependence of $S_{ZFC}(t)$ at T , where t_w is changed as a parameter. (a) $T = 7$ K and $t_w = 2.0 \times 10^3$, 1.0×10^4 , and 3.0×10^4 sec. (b) $T = 8$ K and $t_w = 5.0 \times 10^3$, 1.0×10^4 and 3.0×10^4 sec.

teristics of both ordered and disordered states, because of the following reasons. As shown in Fig. 11(c), ΔM_{ir}^{TRM} is positive (or $M_i > M_r$) for $T_r < T_{cl}$. It becomes zero when T_r is nearly equal to T_{cl} , and takes a negative local minimum at $T_r = T_{cu}$. The disordered nature of the intermediate state is characterized by the negative value of ΔM_{ir}^{TRM} (or $M_i < M_r$). Thus the intermediate state is a sort of disordered state. This feature is in contrast to that of $\Delta M_{ir}^{TRM} > 0$ for a ferromagnetic state of normal ferromagnets. However, the intermediate state also exhibits a memory effect which is one of the main features of the ordered state. The value of M_{TRM} at T_r almost remains unchanged after the cooling process from T_r to T_i and the heating process from T_i to T_r . In this sense, the intermediate state is a sort of ordered state: SG ordered phase extending over ferromagnetic islands (see Sec. III A).

(ii) *ZFC case*. Before the ZFC magnetization measurement, a zero-field cooling (ZFC) protocol was carried out. It consists of the following process, (a) annealing of the system at 50 K for 1200 sec in the absence of H , (b)

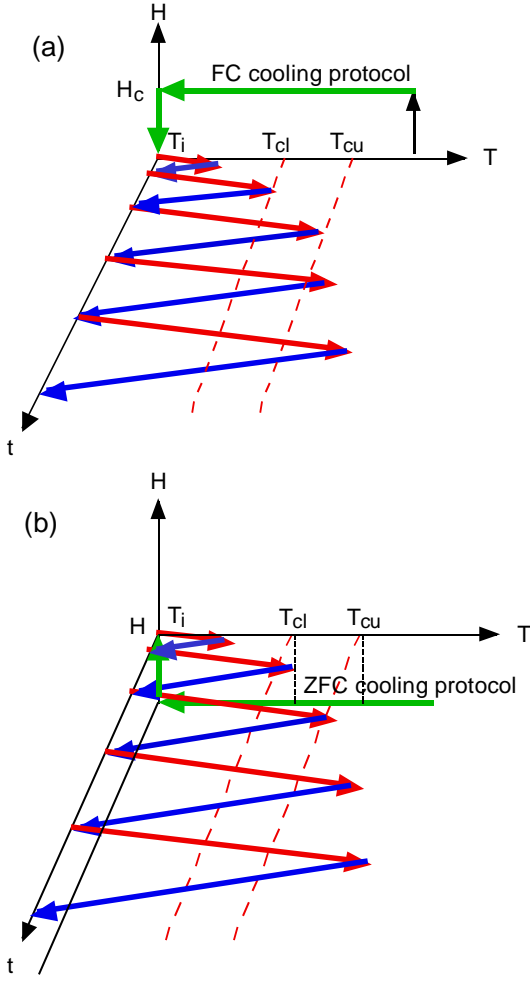


FIG. 7: (Color online) (a) TRM case. Repeated processes of heating from $T_i = 3$ K to T_r (U-turn temperature), cooling from T_r to 3 K, and reheating from T_i K to T_{r+1} ($> T_r$) in the absence of H , after the FC cooling protocol (quenching from 50 K to T_i at $H = H_c = 1$ Oe and annealing at T_i for 100 sec). (b) ZFC case. Repeated processes of heating from $T_i = 3$ K to T_r (U-turn temperature), cooling from T_r to 3 K, and reheating from T_i to T_{r+1} ($> T_r$) in the presence of $H (= 1$ Oe), after the ZFC cooling protocol (quenching from 50 K to T_i at $H = 0$ and aging at T_i for 100 sec).

quenching of the system from 50 K to $T_i = 3$ K, and (c) aging at T_i and $H = 0$ for a wait time $t_w = 100$ sec. Just after the magnetic field ($H = 1$ Oe) is applied to the system, the ZFC magnetization M_{ZFC} was measured using the same procedure of heating and cooling: $T_i \rightarrow T_1 \rightarrow T_i \rightarrow T_2 \rightarrow T_i \rightarrow T_3 \rightarrow T_i \rightarrow$ and so on, where T_r ($r = 1, 2, \dots$) is the U-turn temperature and $T_r > T_i$. The schematic diagram of these processes is shown in Fig. 7(b). Figures 13(a) and (b) show the T dependence of M_{ZFC} using the above method. Note that the value of M_{ZFC} lies between those of M_{ZFC}^{ref} and M_{FC}^{ref} at any T below T_{cu} . Here M_{ZFC}^{ref} is measured with increasing T from T_i to 12 K at $H = 1$ Oe after the ZFC cooling protocol. The magnetization M_{FC}^{ref} is measured

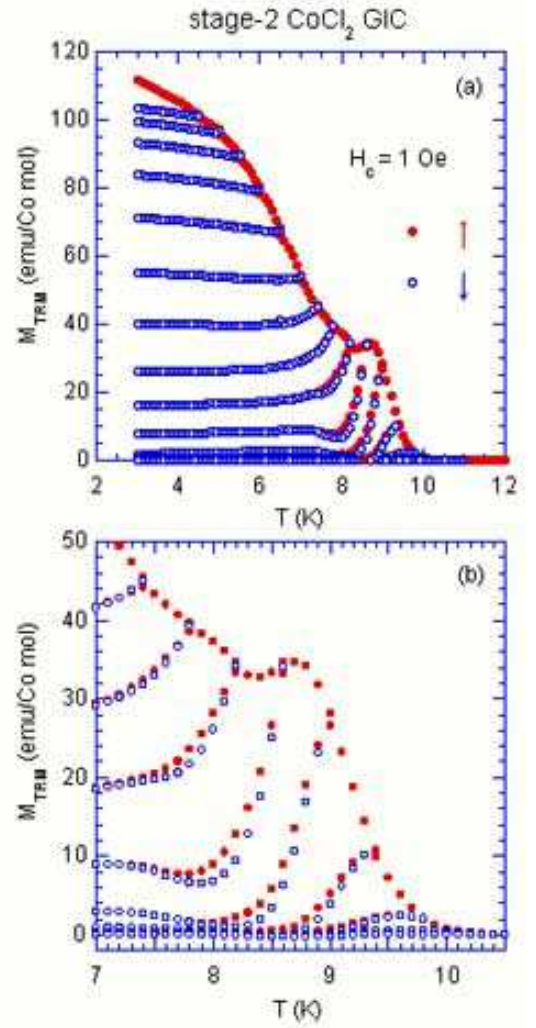


FIG. 8: (Color online) (a) and (b) T dependence of M_{TRM} measured at $H = 0$ in a series of heating (closed circles) and cooling (open circles) process [see Fig. 7(a) and text for detail] after the FC cooling of the system from 50 to $T_i = 3$ K in the presence of $H_c (= 1$ Oe). Note the data of M_{TRM} shown here is a corrected one by the subtraction of the original data from the M_{FC} part under the remnant magnetic field (≈ 5 m Oe).

with decreasing T from 12 K to T_i in the presence of $H (= 1$ Oe). Figure 14 shows typical examples of the path of M_{ZFC} vs T obtained in both the cooling process ($T = T_r \rightarrow T_i$) and the heating process ($T = T_i \rightarrow T_r$), where $T_r = 7.8, 8.2, 8.6,$ and 9.0 K. For $T_r \leq 7.4$ K, the path of $M_{ZFC}(T \downarrow)$ in the cooling process ($T = T_r \rightarrow T_i$) is the same as that of $M_{ZFC}(T \uparrow)$ in the heating process ($T = T_i \rightarrow T_r$), indicating that M_{ZFC} vs T curve is reversible on cooling and heating. For $T_r \geq 7.8$ K, however, the $M_{ZFC}(T)$ curve is irreversible in the cooling and heating processes. For $T_r \geq 9.2$ K, both the path of $M_{ZFC}(T \downarrow)$ in the cooling process ($T = T_r \rightarrow T_i$) and the path of $M_{ZFC}(T \uparrow)$ in the heating process ($T = T_i \rightarrow T_r$) coincide with that of M_{FC}^{ref} which is obtained by cooling

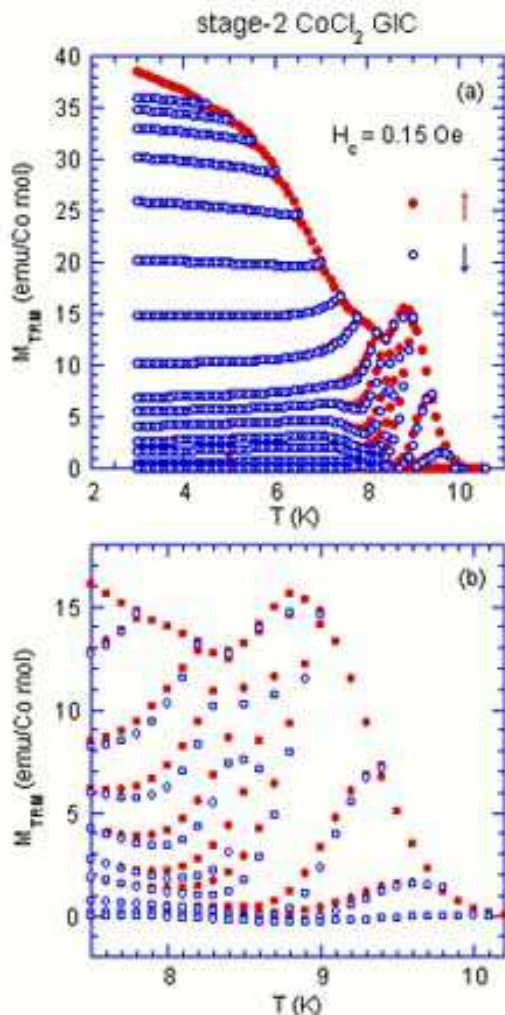


FIG. 9: (Color online) (a) and (b) T dependence of M_{TRM} measured at $H = 0$ in a series of heating (closed circles) and cooling (open circles) processes [see Fig. 7(a) and the text for detail], after the FC cooling of the system from 50 to $T_i = 3$ K in the presence of $H_c (= 0.15$ Oe). Note the data of M_{TRM} shown here is a corrected one by the subtraction of the original data from the M_{FC} part under the remnant magnetic field (≈ 5 mOe).

from the PM phase to $T = T_i$ in the presence of $H (= 1$ Oe).

Figure 15 (a) shows the T_r dependence of M_r and M_i , where M_r and M_i are the values of M_{ZFC} at $T = T_r$ and T_i in the cooling process ($T = T_r \rightarrow T_i$), respectively. Figure 15(b) shows the T_r dependence of the derivative dM_i/dT_r . It exhibits a local maximum at $T_r = T_{cl} = 7$ K. Figure 15(c) shows the difference $\Delta M_{ir}^{ZFC} (= M_i - M_r)$ which is derived from Fig. 15(a). For $T_r < T_{cl}$, ΔM_{ir}^{ZFC} is positive but is nearly equal to zero: $M_i \approx M_r$. At $T_r = T_{cl}$, ΔM_{ir}^{ZFC} starts to increase with increasing T_r . At $T_r \approx 8.2$ K where M_r exhibits a peak, ΔM_{ir}^{ZFC} drastically increases with further increasing T_r . For $T_r > T_{cu}$, M_i reaches the equilibrium value. Note that M_i is 56%

value at $T_r = T_{cl}$ and 98% at $T_r = T_{cu}$ of the equilibrium value. This result also supports that the intermediate state has the nature of the ordered state.

Figure 12(b) shows the difference $\Delta M_{ZFC} [= M_{ZFC}(T\uparrow) - M_{ZFC}(T\downarrow)]$ as a function of T for various T_r . The difference ΔM_{ZFC} exhibits a negative local minimum at a characteristic temperature T_p^{ZFC} below T_r . The T dependence of ΔM_{ZFC} is almost the same that of $-\Delta M_{TRM}$. Note that T_p^{ZFC} for the ZFC process is exactly the same as T_p^{TRM} for the TRM process at the same T_r . In other words, the magnetization gained in the TRM process corresponds to the magnetization lost in the ZFC process. This result supports the fundamental relation

$$M_{ZFC}(t_w, t) = M_{FC}(0, t + t_w) - M_{TRM}(t_w, t), \quad (2)$$

between the time relaxation of TRM, FC, and ZFC magnetization at low H in SG's.²⁰ Similar behavior is observed in the genuine TRM and ZFC measurements of spin glass Ag(11 at % Mn).¹⁶

E. Memory effect for M_{FC}

We present a peculiar memory effect observed in our system using a unique FC cooling protocol. Similar behavior is observed in spin glasses and superparamagnets.^{12,21} The result is shown in Fig. 16. First our system was cooled through the FC cooling protocol from 50 K to intermittent stop temperatures $T_s (= 8.5, 6.5, 4.5$ K) in the presence of $H_c = 1$ Oe. When the system was cooled down to each T_s , the field was cut off ($H = 0$) and aged at T_s for $t_w (= 3.0 \times 10^4$ sec). In this case, the magnetization $M_{FC}^{IS}(T\downarrow)$ decreases with time due to the relaxation. After the wait time t_w at T_s , the field ($H_c = 1$ Oe) was applied again and the FC cooling process was resumed. Such a FC cooling process leads to a step-like behavior of $M_{FC}^{IS}(T\downarrow)$ curve. The value of $M_{FC}^{IS}(T\downarrow)$ after resuming below the lowest stop temperature behaves almost in parallel to that of the FC magnetization without the intermittent stops (as reference curve). After reaching 1.9 K, the magnetization $M_{FC}^{IS}(T\uparrow)$ was measured in the presence of $H (= 1$ Oe) as the temperature is increased at the constant rate (0.05 K/min). The magnetization $M_{FC}^{IS}(T\downarrow)$ thus measured exhibits a broad peak at a characteristic temperature $T_a = 5.3$ K and a peak at $T_a = 7.9$ K. The spin configuration imprinted at the intermittent stop at T_s for a wait time t_w at $H = 0$ during the FC cooling process strongly affects the T dependence of $M_{FC}^{IS}(T\uparrow)$ when the temperature is increased, exhibiting a peculiar memory effect. Figure 16(c) shows the T dependence of the difference ΔM_{FC}^{IS} between $M_{FC}^{IS}(T\uparrow)$ and $M_{FC}^{IS}(T\downarrow)$. Such an oscillatory behavior in ΔM_{FC}^{IS} has been reported in superparamagnets, superspin glasses, and spin glasses. Sasaki et al.²¹ have shown that the aging and memory effects originate solely from a broad distribution of relaxation times. This

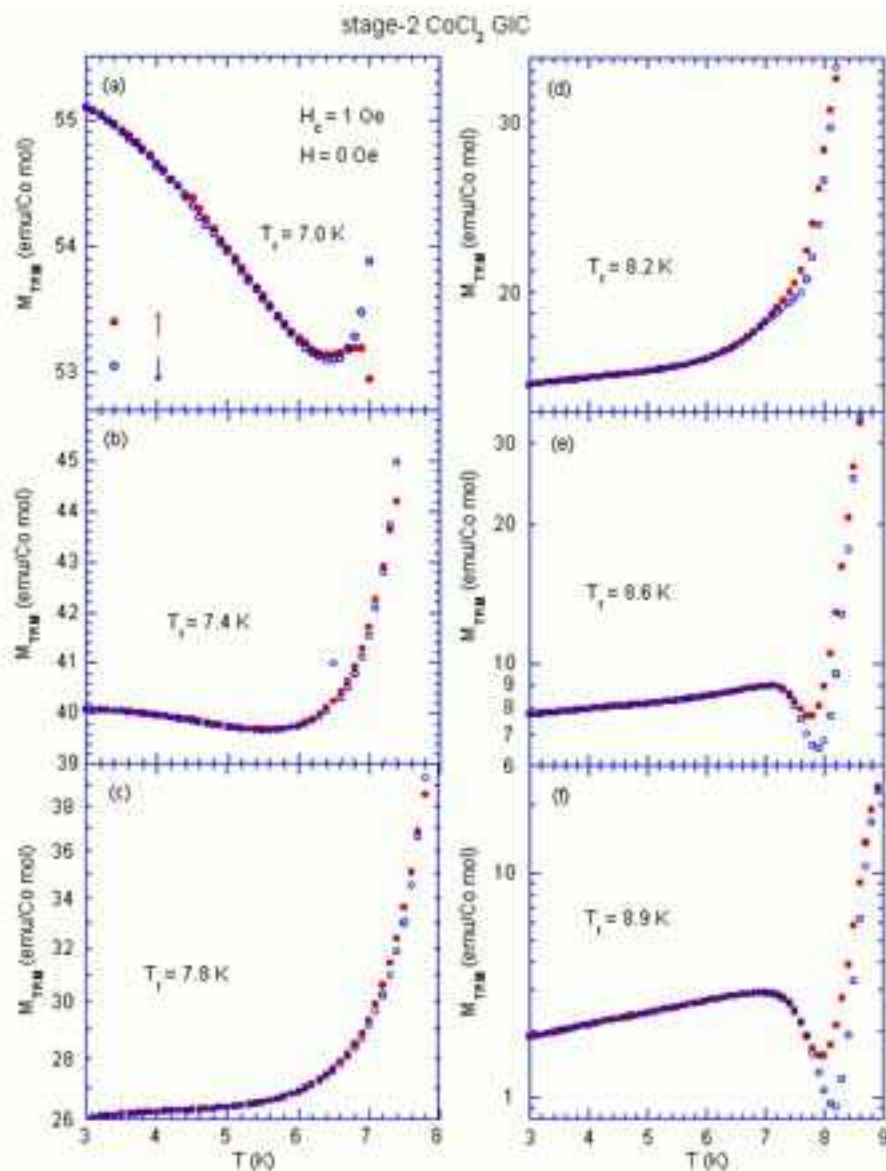


FIG. 10: (Color online) T dependence of M_{TRM} at $H = 0$ which is measured with decreasing T from T_r to $T_i = 3$ K [$M_{TRM}(T\downarrow)$, open circles] and subsequently measured with increasing T from T_i to T_r [$M_{TRM}(T\uparrow)$, closed circles]. (a) $T_r = 7.0$ K, (b) 7.4 K, (c) 7.8 K, (d) 8.2 K, (e) 8.6 K, and (f) 8.9 K.

model may be true for the SG phase extending over ferromagnetic islands. When the field is cut off at $T = T_s$ for $t_s (= 3 \times 10^4$ sec), the magnetic moments of the system formed of small islands whose relaxation times are longer than t_s are frozen in when the cooling is restarted. These frozen states are reactivated when the system is reheated at T_s .

IV. DISCUSSION

A. Ordered and disordered nature of intermediate state

From our result on the memory effect for M_{TRM} presented in Sec. III D, we find that the intermediate state between T_{cl} and T_{cu} has characteristics of both ordered and disordered states. The disordered nature of the intermediate state is characterized by the negative value of ΔM_{ir}^{TRM} (or $M_i < M_r$). This feature is in contrast to that of $\Delta M_{ir}^{TRM} > 0$ for a ferromagnetic state of normal ferromagnets. However, the intermediate state also ex-

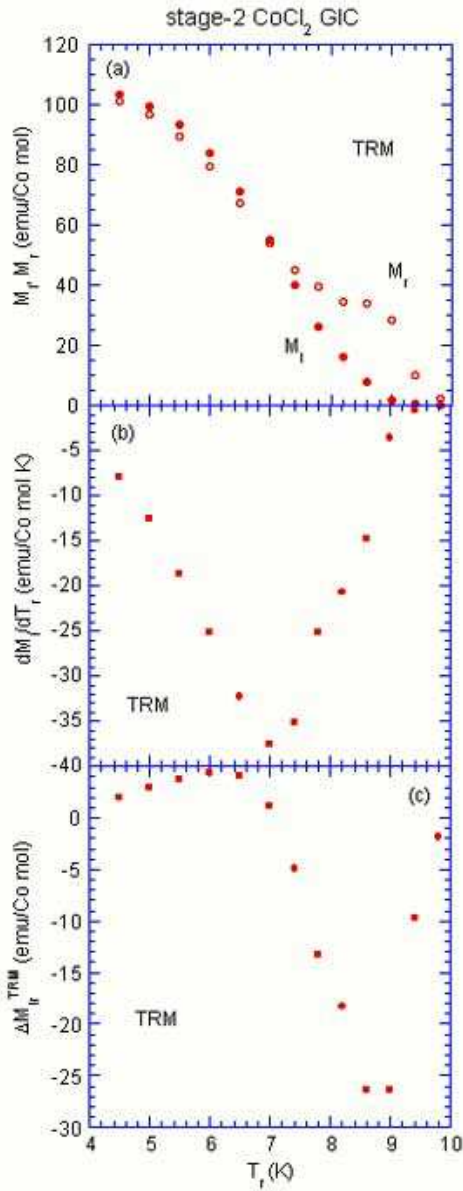


FIG. 11: (Color online) (a) T_r dependence of M_r and M_i . M_r and M_i are the value of M_{TRM} at $T = T_r$ and T_i ($= 3$ K), respectively, which are obtained in the measurement of M_{TRM} with decreasing T from T_r to T_i [see Fig. 8(a)]. (b) T_r dependence of dM_i/dT_r . (c) T_r dependence of ΔM_i^{TRM} ($= M_i - M_r$).

hibits a memory effect as an ordered state. The value of M_{TRM} at T_r almost remains unchanged after the cooling process from T_r to T_i and the heating process from T_i to T_r . In this sense, the intermediate is a sort of ordered state. Such a characteristic phenomenon is explained in terms of intermediate state with intrainland-order and partial interisland-order. But if the intermediate state is a completely interisland-disorder state, then thermal equilibrium M_{TRM} in the state should be always zero. The memory effects observed here indicates that the in-

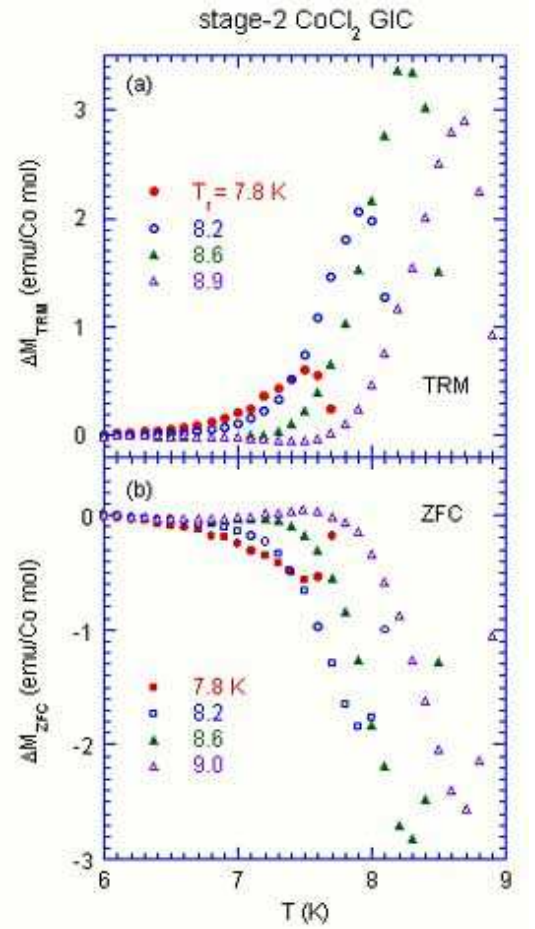


FIG. 12: (Color online) (a) T dependence of ΔM_{TRM} [$= M_{TRM}(T\uparrow) - M_{TRM}(T\downarrow)$] for $7 \text{ K} \leq T \leq T_r$. $T_r = 7.8, 8.2, 8.6,$ and 8.9 K. (b) T dependence of ΔM_{ZFC} [$= M_{ZFC}(T\uparrow) - M_{ZFC}(T\downarrow)$] for $7 \text{ K} \leq T \leq T_r$. $T_r = 7.8, 8.2, 8.6,$ and 9.0 K.

intermediate state is a SG phase extending over islands, where each island is ferromagnetically ordered. The observed characteristic two-step ordering could be understood thermodynamically as a hierarchy one that the SG phase extending over islands occurs at T_{cu} and the 3D order occurs at T_{cl} as an equilibrium state, due to the enhanced interplanar interaction.

B. The domain size from the relaxation rate

$$S_{ZFC}(t)$$

The aging behavior of the intermediate state after the ZFC aging protocol can be understood in terms of the droplet model.^{13,14,15} This ZFC aging protocol process to the intermediate state is completed at $t_a = 0$, where t_a is defined as an age (the total time after the ZFC aging protocol process). Then the system is aged at T under $H = 0$ until $t_a = t_w$, where t_w is a wait time. Correspondingly, the size of domain defined by $R_T(t_a)$ grows with

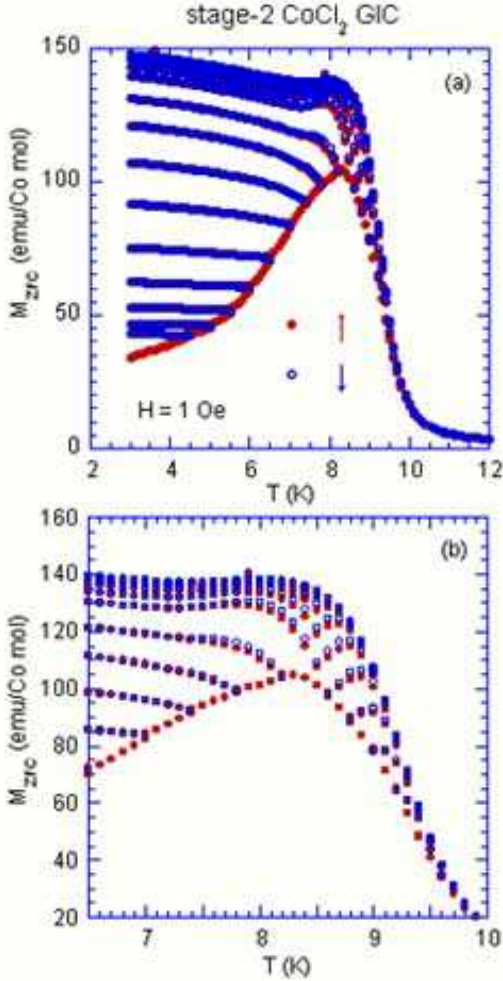


FIG. 13: (Color online) (a) and (b) T dependence of M_{ZFC} measured at $H = 1$ Oe in a series of heating (closed circles) and cooling (open circles) processes [see Fig. 7(b) and the text for detail], after the ZFC cooling of the system from 50 to 3 K in the absence of H .

the age of t_a and reaches $R_T(t_w)$ just before the field is turned on at $t = 0$ or $t_a = t_w$. The aging behavior in M_{ZFC} is observed as a function of the observation time t . After $t = 0$, a probing length $L_T(t)$ corresponding to the maximum size of excitation grows with t , in a similar way as $R_T(t_a)$. When $L_T(t) \ll R_T(t_w)$, quasi-equilibrium dynamics is probed, but when $L_T(t) \gg R_T(t_w)$, non-equilibrium dynamics is probed. It is theoretically predicted that the mean domain-size $L_T(T)$ is described by a power law given by

$$L_T(t)/L_0 \approx (t/t_0)^{1/z(T)}, \quad (3)$$

where L_0 and t_0 are microscopic length and time scale and the T -dependent exponent $z(T)$. It is predicted that the relaxation rate $S_{ZFC}(t)$ exhibits a peak when $L_T(t) \approx R_T(t_w)$.²²

In Sec. III C we show that $S_{ZFC}(t)$ exhibits two peak at $t = t_{cr1}$ and at $t = t_{cr2}$ in the intermediate state. Here

the time t_{cr1} is much shorter than t_{cr2} . The characteristic time t_{cr1} is independent of the wait time t_w , while t_{cr2} is linearly dependent on t_w . The existence of t_{cr1} and t_{cr2} suggests that there are two kinds of characteristic domains with sizes $L_T(t = t_{cr1})$ and $L_T(t = t_{cr2})$. The domain size $L_T(t = t_{cr1})$ may correspond to the size of small island. The growth of the in-plane correlation length ξ_a is limited by the size of the small island. In contrast, t_{cr2} tends to increase with increasing t_w . The domain size $L_T(t = t_{cr2})$ is much larger than that of the small island. These domains may be formed of several small islands through the RKKY interactions. This implies that ξ_a is actually much larger than the size of small islands.

C. In-plane spin correlation length from the genuine TRM measurement

Using the fundamental link given by Eq.(3), the time dependence of the relaxation rate $S_{TRM}(t)$ for the TRM magnetization can be obtained from $S_{TRM}(t)$ as $S_{TRM}(t) = -S_{ZFC}(t)$. From the result of Figs. 6(a) and (b), it follows that that $S_{TRM}(t)$ with $t_w = 1.0 \times 10^4$ sec exhibits two negative local minima at t_{cr1} ($= 2.1 \times 10^3$ sec) and t_{cr2} ($= 6.9 \times 10^3$ sec) at 7 K and t_{cr1} ($= 2.0 \times 10^3$ sec) and t_{cr2} ($= 1.12 \times 10^4$ sec) at 8 K. In the genuine TRM measurement (see Sec. III B), the system is aged at $T = T_s$ for $t = t_s = 1.0 \times 10^4$ sec in the presence of $H = H_c$ ($= 1$ Oe). The above result of $S_{TRM}(t)$ with $t_w = 1.0 \times 10^4$ sec indicates that two kinds of domains coexist: domain with small island size and large domains formed of small islands through the inter-island interactions. Since t_{cr2} is on the same order as t_s ($= t_w$) or a little shorter than t_s , the size of ordered domains reaches the in plane spin correlation length $\xi_a(T_s)$ in thermal equilibrium. The ordered domains are frozen in when the cooling is resumed. These frozen states are reactivated when the system is reheated at T_s . The magnetization $\Delta M_{TRM}(T = T_s; T_s, t_s)$ is approximated by $g_a \mu_B S [\xi_a(T_s)/a]^2$, where g_a ($= 6.4$) is the Landé g -factor of Co^{2+} spin along the a axis in the c plane, S ($= 1/2$) is a fictitious spin, and a is the in-plane lattice constant.¹ As shown in Fig. 4(a), $(\Delta M_{TRM})_{max}$ increases with decreasing T_s from T_{cu} to T_{cl} . Correspondingly $\xi_a(T_s)$ increases with increasing T_s and tends to diverge at $T = T_{cl}$.

D. Overlap length from the genuine TRM measurement

Here we discuss the effect of the overlap length on the genuine TRM magnetization (Sec. III B). The ordered domains generated at $T = T_s$ are frozen in and survives the spin reconfiguration occurring at lower temperature on shorter length scales. The rejuvenation of the system occurs as the temperature is decreased away from T_s .

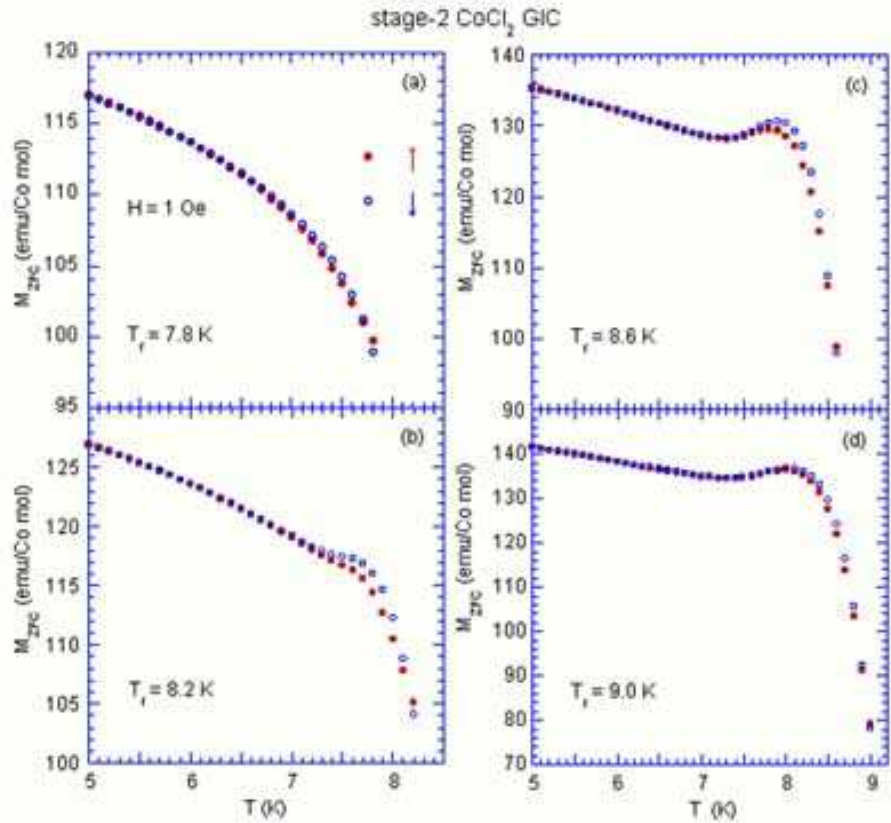


FIG. 14: (Color online) T dependence of M_{ZFC} at $H = 1$ Oe measured with decreasing T from T_r to T_i ($= 3$ K) [$M_{ZFC}(T\downarrow)$, open circles] and subsequently measured with increasing T from T_i to T_r [$M_{ZFC}(T\uparrow)$, closed circles]. (a) $T_r = 7.8$, (b) 8.2, (c) 8.6, and (d) 8.9 K.

The spin configuration imprinted at T_s is recovered on reheating. In this sense, the system sustains a memory of an equilibrium state reached after a stop-wait process at T_s . The influence of the spin configuration imprinted at a stop-wait protocol is limited to a restricted temperature range around T_s on reheating. The width of this region may be assigned to the existence of an overlap between the spin configuration attained at T_s and the corresponding state at a very neighboring temperature ($T_s + \Delta T$).

Here we introduce a concept of the overlap which is encountered in the SG system.^{13,14,15} The SG equilibrium configurations at different temperatures at T and $T + \Delta T$ are strongly correlated only up to the overlap length $L_{\Delta T}$, beyond which these correlations decay to zero. From the droplet theory, the overlap length $L_{\Delta T}$ is described by

$$L_{\Delta T}/L_0 \approx (T^{1/2}|\Delta T|/\Upsilon_T^{3/2})^{-1/\zeta}, \quad (4)$$

where ζ is the chaos exponent ($\zeta = d_s/2 - \theta$), d_s is the fractal dimension of the surface of the droplet, and Υ_T is the temperature corresponding to the wall stiffness Υ . The overlap length decreases with increasing $|\Delta T|$. The width ΔT is determined from the condition that $R_{T_s}(t_s) = L_{\Delta T}$.

In our system, the spin configuration imprinted during

the stop-wait protocol at $T = T_s$ for $t = t_s$ is unaffected by a small temperature shift such that the overlap length $L_{\Delta T}$ is larger than the average domain sizes. There is a sufficient overlap between the equilibrium spin configurations at the two temperatures T_s and $T_s + \Delta T$. The situation is different when the temperature shift becomes large. The overlap length becomes shorter than the original domain sizes. A smaller overlap between spin configurations promotes the formation of broken domains. When the temperature shift is sufficiently large, the overlap length is much shorter than the original domain sizes, leading to the rejuvenation of the system.^{22,23,24,25} The asymmetric form of $\Delta M_{TRM}(T; T_s, t_s)$ around $T = T_s$ ($= 7.6$ K) between T_{cl} and T_{cu} indicates that the spin configuration under the positive T -shift is different from that under the negative T -shift. The domain size of the partial SG phase may drastically increase with decreasing T below $T = 7.6$ K, partly because of enhanced interisland interactions.

V. CONCLUSION

We have studied the aging dynamics of stage-2 CoCl_2 GIC between two magnetic phase transitions at T_{cl} ($= 7.0$

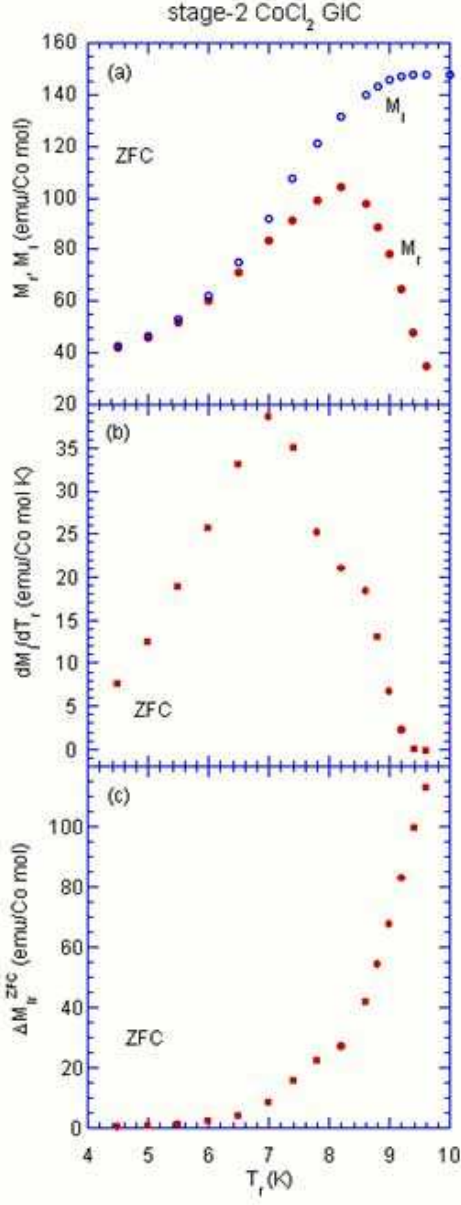


FIG. 15: (Color online) (a) T_r dependence of M_r and M_i . M_r and M_i are the value of M_{ZFC} at $T = T_r$ and T_i ($= 3$ K), respectively, which are obtained in the measurement of M_{ZFC} with decreasing T from T_r to T_i [see Fig. 12(a)]. (b) T_r dependence of dM_i/dT_r . (c) T_r dependence of ΔM_{ir}^{ZFC} ($= M_i - M_r$).

K) and T_{cu} ($= 8.9$ K). The observed aging phenomena is well explained within the framework of the droplet model for SG systems. The intermediate state between T_{cl} and T_{cu} has characteristic of both ordered and disordered states. A genuine thermoremanent magnetization (TRM) measurement indicates that the memory of the specific spin configurations imprinted at temperatures between T_{cl} and T_{cu} during the field-cooled (FC) aging protocol can be recalled when the system is re-heated at a constant heating rate. The zero-field cooled (ZFC) and TRM

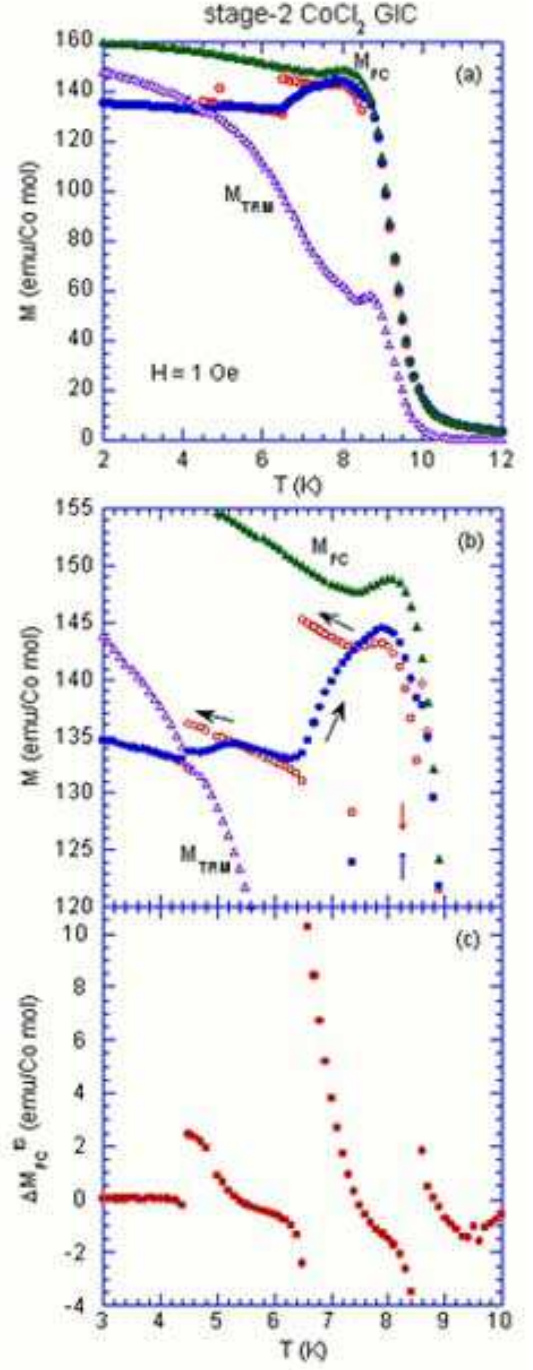


FIG. 16: (Color online) (a) and (b) T dependence of $M_{FC}^{IS}(T\downarrow)$ and $M_{FC}^{IS}(T\uparrow)$ observed in the following FC cooling protocol. The system was quenched from 50 to 12 K in the presence of H ($= 1$ Oe). $M_{FC}^{IS}(T\downarrow)$ was measured with decreasing T from 12 to 1.9 K but with intermittent stops at $T = 8.5$, 6.5, and 4.5 K for a wait time $t_w = 3.0 \times 10^4$ sec. The field is cut off during each stop. $M_{FC}^{IS}(T\uparrow)$ was measured at $H = 1$ Oe with increasing T after the above cooling process. The T dependence of M_{FC}^{ref} and M_{TRM}^{ref} are also shown as reference curves. These are measured after the FC cooling protocol without intermittent stop (reference curves). (c) T dependence of the difference ΔM_{FC}^{IS} [$= M_{FC}^{IS}(T\downarrow) - M_{FC}^{IS}(T\uparrow)$].

magnetization is examined in a series of heating and re-heating process. The magnetization shows both characteristic memory and rejuvenation effects. The time (t) dependence of the relaxation rate $S_{ZFC}(t)$ after the ZFC aging protocol with a wait time t_w , exhibits two peaks at characteristic times t_{cr1} and t_{cr2} between T_{cl} and T_{cu} . An aging process is revealed as the strong t_w dependence of t_{cr2} . These results suggest that two types of ordered domains coexist in the intermediate state. The intermediate state is a SG phase extending over ferromagnetic islands.

Below T_{cl} , the interplanar interaction between islands in adjacent intercalate layers becomes strong, leading to the 3D ordered phase.

Acknowledgments

The authors would like to thank H. Suematsu for providing them with single crystal of kish graphite.

-
- * suzuki@binghamton.edu
 † itsuko@binghamton.edu
- ¹ T. Enoki, M. Suzuki, and M. Endo, *Graphite Intercalation Compounds and Applications* (Oxford University Press, Oxford, 2003). Chapter 7. p.236. See also references therein.
 - ² Y. Murakami, M. Matsuura, M. Suzuki, and H. Ikeda, *J. Magn. Magn. Mater.* **31-34**, 1171 (1983).
 - ³ M. Matsuura, Y. Endoh, T. Kataoka, and Y. Murakami, *J. Phys. Soc. Jpn.* **56**, 2233 (1987).
 - ⁴ D.G. Wiesler, M. Suzuki, and H. Zabel, *Phys. Rev. B* **36**, 7051 (1987).
 - ⁵ M. Matsuura, N. Tanaka, Y. Karaki, and Y. Murakami, *Japanese J. Appl. Phys.* **26-S3**, 797 (1987).
 - ⁶ Y. Murakami and M. Matsuura, *J. Phys. Soc. Jpn.* **57**, 1056 (1988).
 - ⁷ M. Matsuura and M. Hagiwara, *J. Phys. Soc. Jpn.* **59**, 3819 (1990).
 - ⁸ M. Matsuura, Y. Murakami, and M. Hagiwara, *Physica A* **191**, 316 (1992).
 - ⁹ K. Miyoshi, M. Hagiwara, and M. Matsuura, *J. Phys. Soc. Jpn.* **65**, 3306 (1996).
 - ¹⁰ M. Suzuki and I.S. Suzuki, *Phys. Rev. B* **58**, 840 (1998).
 - ¹¹ M. Suzuki, I.S. Suzuki, and T.-Y. Huang, *J. Phys. Condens. Matter* **14**, 5583 (2002).
 - ¹² Y. Sun, M.B. Salamon, K. Garnier, and R.S. Averback, *Phys. Rev. Lett.* **91**, 167206 (2003).
 - ¹³ D.S. Fisher and D.A. Huse, *Phys. Rev. Lett.* **56**, 1601 (1986).
 - ¹⁴ A.J. Bray and M.A. Moore, *Phys. Rev. Lett.* **58**, 57 (1987).
 - ¹⁵ D.S. Fisher and D.A. Huse, *Phys. Rev. B* **38**, 373 (1988); **38**, 386 (1988); **43**, 10728 (1991).
 - ¹⁶ R. Mathieu, P.E. Jönsson, D.N.H. Nam, and P. Nordblad, *Phys. Rev. B* **63**, 092401 (2001).
 - ¹⁷ R. Mathieu, P.E. Jönsson, P. Nordblad, H. Aruga Katori, and A. Ito, *Phys. Rev. B* **65**, 012411 (2001).
 - ¹⁸ S. Sahoo, O. Petravic, W. Kleemann, P. Nordblad, S. Cardoso, and P.P. Freitas, *Phys. Rev. B* **67**, 214422 (2003).
 - ¹⁹ S. Sahoo, O. Petravic, W. Kleemann, S. Stappert, G. Dumpich, P. Nordblad, S. Cardoso, and P.P. Freitas, *Applied Phys. Lett.* **82**, 4116 (2003).
 - ²⁰ C. Djurberg, J. Mattsson, and P. Nordblad, *Europhys. Lett.* **29**, 163 (1995).
 - ²¹ M. Sasaki, P.E. Jönsson, H. Takayama, and H. Mamiya, *Phys. Rev. B* **71**, 104405 (2005).
 - ²² L. Lundgren, in *Relaxation in Complex Systems and Related Topics*, edited by I.A. Campbell and C. Giovannella (Plenum Press, New York, 1990) p.3.
 - ²³ P. Granberg, L. Sandlund, P. Nordblad, P. Svedlindh, and L. Lundgren, *Phys. Rev. B* **38**, 7097 (1988).
 - ²⁴ P.E. Jönsson, H. Yoshino, and P. Nordblad, *Phys. Rev. Lett.* **89**, 097201 (2002).
 - ²⁵ M. Suzuki and I.S. Suzuki, *Eur. Phys. J. B*, **41**, 457 (2004).